



Nanoscale

Tuning the Photodynamics of Sub-nanometer Neutral Chromium Oxide Clusters Through Sequential Oxidation

Journal:	<i>Nanoscale</i>
Manuscript ID	NR-ART-01-2022-000464.R2
Article Type:	Paper
Date Submitted by the Author:	13-Apr-2022
Complete List of Authors:	Garcia, Jacob; Arizona State University, School of Molecular Sciences Sayres, Scott; Arizona State University, School of Molecular Sciences

SCHOLARONE™
Manuscripts

ARTICLE

Tuning the Photodynamics of Sub-nanometer Neutral Chromium Oxide Clusters Through Sequential Oxidation

Jacob M. Garcia^{ab} and Scott G. Sayres^{ab*}

Received 00th January 20xx,
Accepted 00th January 20xx

DOI: 10.1039/x0xx00000x

Sub-nanometer neutral chromium oxide clusters were produced in the gas phase through laser ablation and their low-lying excited state lifetimes were measured using femtosecond pump-probe spectroscopy. Time-dependent density functional theory calculations relate the trends in experimental lifetimes to the cluster's electronic structure. The photoexcited $(\text{CrO}_2)_n$ ($n < 5$) cluster transients with the absence of up to four O atoms ($\text{Cr}_n\text{O}_{2n-x}$, $x < 5$) exhibit a ~ 30 fs and sub-ps lifetime, attributed to instantaneous metallic e-e scattering and vibrationally mediated charge carrier relaxation, respectively. A long-lived (> 2 ps) response is found in both small and clusters with low O content, indicating that terminal Cr=O bonds facilitate efficient excited state relaxation. The ~ 30 fs transient signal fraction grows nearly linearly with oxidation, matching the amount of O-2p to Cr-3d charge transfer character of the photoexcitation and suggesting a gradual transition between semiconducting and metallic behavior in chromium oxide clusters at the molecular level. The results presented herein suggest that the photocatalytic properties of chromium oxides can be tunable based on size and oxidation.

1 Introduction

Chromium oxides are widely studied materials for their interesting magnetic and catalytic properties. They have been recently examined for solar cells,¹ CO_2 dissociation,² activation of methane,³ and magnetic and spintronic devices.⁴ One of the common bulk forms of chromium oxide, CrO_2 , has a rutile structure and unusual metallic and ferromagnetic characteristics compared to most metal oxides, which are nonmetallic and antiferromagnetic. The well-established half-metallic property and highest spin polarization of CrO_2 over any other material^{5–7} has attracted strong interest for spintronics and data storage. The half-metallic properties of CrO_2 arise from a direct band gap of 1.8 eV in a spin-down configuration and metallic behavior in spin-up configurations.⁷ The other stable bulk oxide, Cr_2O_3 , has a more stable stoichiometry, assumes a corundum-type structure with octahedral metal centers forming t_{2g} and e_g bands, and is a wide bandgap antiferromagnetic insulator ($E_g = 3.4$ eV).^{8,9} Below the absorption edge, two other weak optical transitions appear at ~ 2 and ~ 2.6 eV,^{10,11} usually attributed to d-d transitions. The partially filled, spin-polarized 3d shell makes chromium oxide materials interesting and has led to numerous investigations on the manipulation of electronic and magnetic states.

Controlling and inducing magnetic states requires in-depth information on both the oxygen-dependent electronic states

and the different mechanisms for which they transport energy. Ultimately, the timeframe to induce magnetic and chemical change relies on the ability to produce excited states which survive for long periods of time and may be examined with atomic precision using clusters. Clusters of specific atomic composition allow for investigations on the effects of atomic changes to electronic properties. In addition, chromium oxide clusters may be uniquely suitable for spintronics due to an array of energetically competitive spin isomers. The magnetic superexchange interactions in many clusters can reach extreme magnetic values, such as a high total spin magnetic moment of up to 11 μ_B for Cr_3O_3^+ .¹² This antiferromagnetic coupling weakens with oxidation and is expected to eventually quench when fully coordinated in the $(\text{CrO}_3)_n$ stoichiometry. Therefore, the suboxide clusters exhibit the most interesting phenomena.

Chromium oxides have electronic configurations that arise from a unique mixing of half-filled Cr s- and d-orbitals with O 2p-orbitals. The electronic bonding and states of Cr and O have been extensively explored in CrO .^{13–19} Photoelectron spectroscopy (PES) revealed multiple excited states of CrO_2 ^{18,20–22} and supported by theory.^{23,24} In particular, Cr_2O_n clusters have been heavily studied both experimentally and theoretically,^{25–29} showing large changes in electronic structure with oxygen content via photoelectron spectroscopy (PES),^{25,28,29} and structures in agreement with vibrationally resolved IR spectroscopy.^{30–32} Only a few measurements have determined the properties of chromium oxide clusters containing several metal atoms.^{8,12,33–37}

Our recent work on the transient dynamics of Cr_2O_n ($n < 5$) clusters revealed an increased metallic-like relaxation mechanism with higher O content,³⁸ related to the percent ligand-to-metal charge-transfer (LMCT) character of the photoexcitation.³⁸ However, larger chromium oxides need to be

^a School of Molecular Sciences, Arizona State University, Tempe, AZ 85287

^b Biodesign Center for Applied Structural Discovery, Arizona State University, Tempe, AZ 85287

*E-mail: Scott.Sayres@asu.edu

Electronic Supplementary Information (ESI) available: Figs. S1–S4 shows the calculated excited state orbital contributions for chromium oxide clusters. See DOI: 10.1039/x0xx00000x

examined to elucidate the connection between excited state lifetimes and electronic transitions as chromium oxides grow in size to explore their potential for material applications. Here, we report the transient dynamics of CrO_n , Cr_3O_n and Cr_4O_n clusters and show how their behavior is nearly consistent with increases in cluster size. This simple study of sequential oxidation and growth of chromium oxide materials reveals new insights into excited state relaxation mechanisms, such as electron-electron (e-e) scattering and metallic behavior, which impact their development as tunable materials for photocatalysis, spintronics, and other industrial applications.

2 Methods

2.1 Cluster Production and Detection

Excited state dynamics of chromium oxide clusters were measured using a home-built Wiley-McLaren³⁹ type time-of-flight mass spectrometer (TOF-MS) coupled to a femtosecond (fs) laser, discussed in detail previously.^{40,41} Briefly, a pulsed 532 nm laser was used to ablate a pure 1/4" Cr rod. The plasma plume was directed by pulsed expansion of 100 psi of He gas seeded with 9% O_2 , confined to a 1 x 60 mm collision region, and then skimmed to a collimated molecular beam diameter of 2 mm. The cations and anions were deflected prior to ionization of the neutral molecular beam by traversing a skimmer charged to +500 V. Clusters were ionized by fs laser pulses and then accelerated by a ~4 kV pulse on the TOF grids. The neutral clusters that were ionized by the sequence of fs laser pulses were focused onto the MCP detector using an Einzel lens and separated in time through a field-free region. Internal pressure of $\sim 7.5 \times 10^{-8}$ Torr was maintained using three high-vacuum turbo pumps and precise synchronization of the laser pulses, pulsed valve, and TOF grids were controlled using two pulse generators in tandem.

2.2 Pump Probe Spectroscopy

A series of fs laser pulses from a Ti:sapphire laser were employed to ionize the neutral clusters for detection through mass spectrometry. A single 400 nm (3.1 eV) pump photon initiates a charge transfer relaxation mechanism in neutral clusters that is probed through ionization by a synchronized strong-field 800 nm (1.55 eV) probe beam. The 800 nm laser pulse was sent through an optical delay-stage and scanned in 40 fs increments from -600 fs to +2.5 ps with respect to the 400 nm pump pulse, with an average of 800 spectra collected at each time-delay. All spectra and dynamics were recorded using a 400 nm pump laser intensity of 4.81×10^{14} W/cm² and 800 nm probe intensity of 3.27×10^{15} W/cm². The powers of both beams were kept at a minimum to reduce ionization from an individual laser pulse and to suppress fragmentation. The pulse width of the 800 nm beam was measured through autocorrelation to be <35 fs. The instrumental response function (Gaussian function) is measured to be < 50 fs (FWHM) using the non-resonant ionization signal of O_2 that matches the cross correlation.

The excited state dynamics of neutral chromium oxide clusters are measured by scanning the optical delay of the

probe beam with respect to the pump pulse and tracking the change of intensity from each ion signal. The transient signal of the clusters is a convolution of the cluster response and the cross-correlation of the two laser beams. Therefore, the maximum intensities of the ion signals are recorded ~50 fs after the temporal overlap of the two laser pulses (time zero) and the temporal shift is proportional to the lifetime of the cluster.

Transient ion signals were fit using a series of exponential decay functions convoluted with a Gaussian function as described in detail previously.^{38,40-42} Two decay functions were used to account for a fast signal ($\tau_1 = 30$ fs) and a sub-picosecond signal lifetime (τ_2). The instantaneous decay (on the time scale of the laser pulse) is attributed to e-e scattering and is shown to be related to the LMCT, or excitation from the O-2p orbitals to the Cr-3d orbitals. The sub-ps relaxation is attributed to vibrational relaxation of the initially formed charge-transfer state (electron-vibration relaxation). A plateau function represents the long-lived signal from an excited state that has a lifetime surviving beyond the scope of this experiment (> 2.5 ps). The fractional amplitude coefficients for the fast (30 fs) fitting function (κ_1), sub-ps lifetime component (κ_2) and plateau (δ) functions of the total signal are compared across clusters with changes in oxidation to reveal trends in the nature of the intermediate excited state and its relaxation mechanism.

2.3 Computational Methods

The ground state geometries of Cr_nO_m clusters were optimized at the density functional theory (DFT) level within the Gaussian16⁴³ software suite using the GGA functional uBPW91⁴⁴ with the standard 6-311G+ (d) basis set [15s11p6d1f/10s7p4d1f for Cr and 12s6p1d/5s4p1d for O], which has been shown to be highly accurate for the structures and energies of chromium oxide clusters.^{23,27,30} The clusters recorded in this distribution avoid both Cr-Cr and O-O bonds. Thus, the clusters with $(\text{CrO})_n$ stoichiometry form ring-like structures, with additional O atoms attaching to the periphery as Cr=O bonds.

The minimum state geometries were used as input for single point time-dependent density functional theory (TD-DFT) calculations to account for the excited state characteristics. However, excited state energies and charge-transfer characters are strongly dependent on the choice of exchange-correlation (XC) potential. A well-known charge transfer (CT) problem exists in TD-DFT, where XC potentials with low percentages of Hartree-Fock-like exchange fail to correctly account for the excitation energies of CT states.⁴⁵ The Coulomb attenuating method (CAM)-B3LYP⁴⁶ balances the local excitation and CT, and has been shown to give accurate results for the excited state energies of TiO_2 ,^{47,48} Cr_2O_x ³⁸ and pure metallic⁴⁹ clusters. Thus, the excited states of each cluster were calculated using TD-DFT with unrestricted CAM-B3LYP using the ground state geometries determined from uBPW91 as input. Only spin-conserved (dipole-allowed) transitions were considered. An excited state population analysis was performed to determine the elemental contributions to the excited state. The photoexcited state CT character for all excited states below 4.0 eV are presented in Fig. S1-S4. The maximum LMCT character

increases linearly with O content, in agreement with the trend in experimental fitting coefficients. The valence orbitals are Cr-3d dominated, with O-2p orbitals becoming important only for high energy excitations or in clusters containing many O atoms. In general, the excited states within a narrow energy range involve similar molecular orbitals. Thus, although the broad bandwidth of the ~ 35 fs pump pulse and large density of states make it difficult to definitively assign the accessed photoexcited state and relaxation pathways, we select the excited state with the largest LMCT value near 3.1 eV for comparison to experimental results.

3. Results and Discussion

3.1 Neutral Cr_nO_m Cluster Distribution

The neutral Cr_nO_m distribution sampled through fs ionization from the combined 400 nm pump and 800 nm probe beam at temporal overlap is shown in Fig. 1. We report the first neutral Cr_nO_m cluster distribution, which demonstrates a preference to form $(\text{CrO}_2)_n$ clusters and suboxides with the absence of up to four O atoms. Chromium oxides of the composition Cr_nO_{2n} to $\text{Cr}_n\text{O}_{2n-4}$ are observed up to $n = 6$. In this neutral cluster distribution, CrO has the highest intensity. The neutral chromium oxide cluster distribution contains several stoichiometries of $\text{Cr}_n\text{O}_{2n-x}$ ($n < 7$, $x = 0-4$) with $\text{Cr}_n\text{O}_{2n-2}$ clusters being dominant. For example, Cr_2O_2 , Cr_3O_4 , and Cr_4O_6 are all particularly intense peaks in the cluster distribution compared to their neighbors.

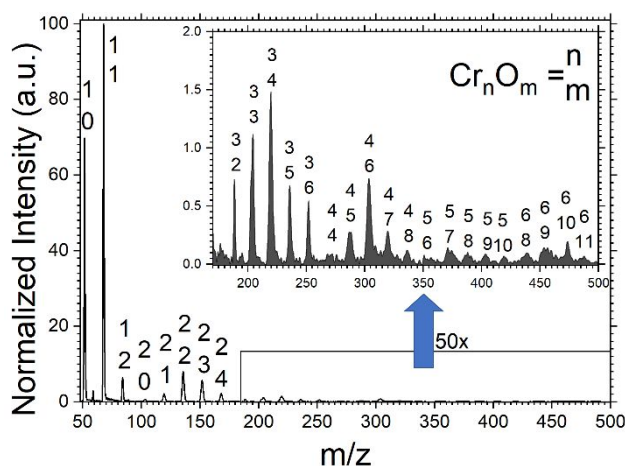


Figure 1: Ionized neutral mass spectrum of chromium oxide clusters at temporal overlap of the pump and probe pulse. The figure inset shows a zoom (50x) of the heavier clusters for clarity.

Typically, gas-phase chromium oxide anion^{8,28,33,37} and cation^{35,50} cluster distributions contain up to the fully coordinated $(\text{CrO}_3)_n$ stoichiometry, which are not recorded here. Such clusters are also considered to be extremely stable and rigid,³⁴ suggesting an upper bound to the cluster's oxidation state. Further, highly oxidized clusters, such as Cr_3O_7^+ and $\text{Cr}_4\text{O}_{10}^+$, have been found to be the dominant stable fragments from the photodissociation of larger clusters.³⁵ The absence of

Table 1: Sub-ps lifetimes (τ_2), total fitting function fraction of the fast (κ_1), sub-ps (κ_2), long-lived (δ) dynamic, and percent LMCT for all neutral $\text{Cr}_n\text{O}_{2n-x}$ ($n < 5$) cluster species.

Series	n	τ_2 (fs)	κ_1	κ_2	δ	LMCT (%)
CrO_n	0	395 ± 38	0.00	0.72	0.28	0
	1	373 ± 39	0.54	0.37	0.09	68
	2	333 ± 52	0.68	0.28	0.04	68
Cr_2O_n	0	346 ± 43	0.00	0.72	0.28	0
	1	620 ± 60	0.33	0.49	0.18	18
	2	499 ± 28	0.56	0.34	0.10	31
	3	413 ± 31	0.70	0.26	0.04	50
Cr_3O_n	4	512 ± 48	0.84	0.16	0.00	63
	3	770 ± 95	0.56	0.41	0.03	5
	4	582 ± 58	0.71	0.25	0.04	37
	5	557 ± 72	0.70	0.28	0.02	33
Cr_4O_n	6	530 ± 94	0.83	0.17	0.00	46
	4	720 ± 127	0.03	0.90	0.07	5
	5	781 ± 73	0.34	0.52	0.14	6
	6	491 ± 29	0.63	0.32	0.05	11
	7	458 ± 74	0.69	0.27	0.04	15
	8	948 ± 311	0.80	0.18	0.02	30

such highly oxidized clusters here is attributed to the low concentration of O_2 employed and not due to fragmentation. Further, the fragmentation energies of the Cr_2O_n clusters ($n = 1-6$) is > 4 eV,²⁷ and are stable to photoexcitation of the pump (3.1 eV) beam. The dissociation energy of CrO_2 is > 5 eV²⁴ supporting the absence of significant fragmentation during the ionization mechanism by the fs lasers used herein.

3.2 Oxidation Effect on Transient Dynamics

In both bulk metals and pure metal clusters,⁵¹⁻⁵³ excess energy dissipates through e-e scattering within 10s of fs due to strong interactions between delocalized electrons. In contrast, electron-hole excitations in semiconductors are typically characterized by longer lifetimes. Sub-nanometer sized systems often contain a large energetic splitting of the molecular orbitals (lower density of states), which greatly reduces relaxation rates and leads to longer lifetimes. However, metallic scattering can dominate if there are many delocalized electrons and a sufficiently high density of states, such as the case in even small clusters. Complete electron transfer is commonly assumed in transition metal oxides, meaning that each O atom removes two d-electrons from the metal atoms. Therefore, adjustments to the cluster's overall oxidation is an effective method to transition between metallic and insulating behavior.

Here, the transient dynamics recorded for chromium oxide clusters demonstrate a strong change in behavior with the addition of O atoms. Specifically, the instantaneous O-2p to Cr-3d e-e scattering processes (κ_1 contribution) increases with oxidation and suggests that chromium oxide clusters become more metallic with increasing oxidation. This counterintuitive result can be understood by considering that the clusters are approaching the stoichiometry of the bulk half-metal, CrO_2 . Each of the chromium oxide cluster series will be described in detail below. All lifetimes and fitting coefficients are presented in Table 1.

The three clusters measured within the CrO_n series ($n = 0-2$) show similar lifetimes of ~ 370 fs (Fig. 2) and a κ_1 contribution that matches the percent LMCT closely. Cr has no O content, resulting in 0% LMCT and has no κ_1 . CrO and CrO_2 both show LMCT increases to over 60% and results in a fast function contribution of 54% and 68% in CrO and CrO_2 , respectively. Although the LMCT character of the photoexcited state is the same for CrO and CrO_2 (68%), the additional terminal O atom in CrO_2 facilitates its faster relaxation resulting in a slightly larger κ_1 (0.68 for CrO_2 and 0.54 for CrO). The LMCT projects electron density back onto the Cr-3d orbitals and induces a rapid scattering on the few-fs timescale similar to metallic behavior of bulk metals. PES experiments on CrO_n ($n = 1-5$) clusters reveals broad excitations in the region ~ 3.1 eV above the neutral ground state.²³ This high density of excited states are attributed to O 2p-derived orbital contributions,²⁴ and in agreement with our calculations that show a strong LMCT character.

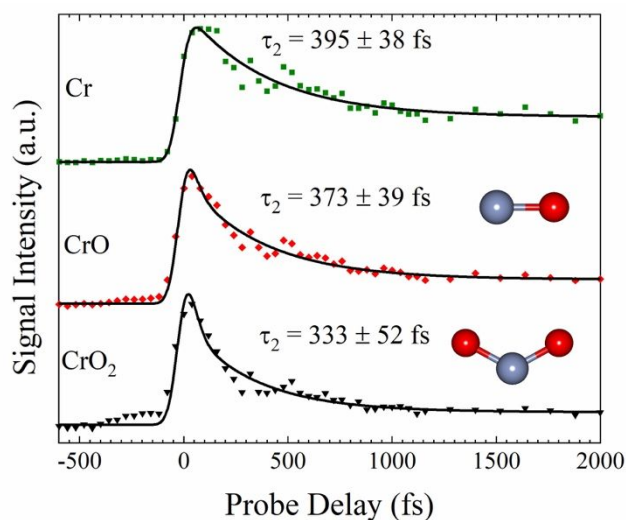


Figure 2: Transient signals of the ionized neutral CrO_n clusters ($n < 3$) with total fit in black and sub-ps lifetime (τ_2) shown next to each cluster.

We previously reported the transient signals of Cr_2O_n ($n < 5$) clusters collected using identical experimental conditions.³⁸ Photoexcitation with a 3.1 eV pump photon shifts from d-d transitions between Cr atoms toward more LMCT behavior in Cr_2O_n clusters as they become more oxidized. The Cr_2 cluster transient response shows only a sub-ps and long-lived response. As O atoms are added, the relative amplitude of the ~ 30 fs response (κ_1) grows nearly linearly, matching the increase in LMCT character of the cluster's excited state. The transient dynamics of Cr_2O_4 contains 84% κ_1 . The nearly linear changes to the various fitting coefficients with addition of O atoms suggests that the ultrafast transient dynamics can be tuned through the oxidation state of the Cr atoms. This system also hinted to the presence of the terminal O atoms being important in driving the LMCT response associated with κ_1 . For example, Cr_2O_4 contains two terminal O atoms²⁷ and its transient dynamics are dominated by κ_1 .

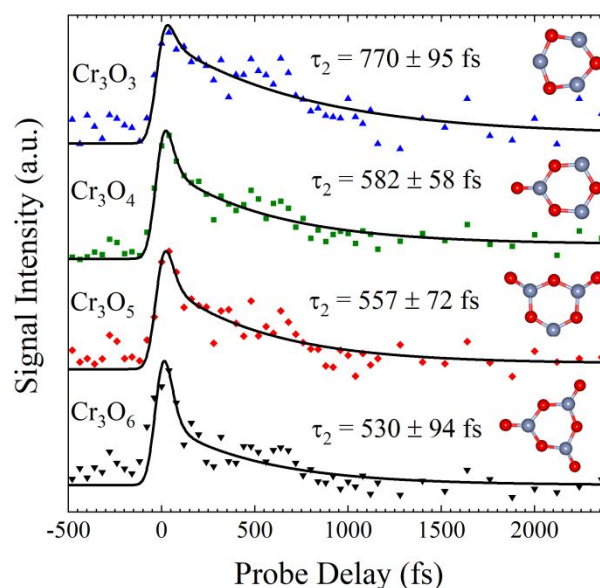


Figure 3: Transient signals for the ionized neutral Cr_3O_n clusters ($n = 3-6$) with total fit in black and sub-ps lifetime (τ_2) shown in each cluster frame.

The transient dynamics and stable structures of Cr_3O_n clusters ($n = 3-6$) are presented in Fig. 3. The lowest energy structures for Cr_3O_n ($n < 7$) clusters are consistent with previous investigations,^{12,36} with Cr_3O_3 forming a ring structure and additional O binding externally to each Cr in planar structures. Upon sequential addition of O atoms in the Cr_3O_n series, the relative κ_1 and κ_2 contributions change, and forms an almost linear trend (Fig 4a). However, the long-lived plateau (δ) component reaches a maximum relative contribution for Cr_3O_4 . Similar to Cr_2O_4 ,³⁸ Cr_3O_6 possesses predominantly a LMCT from the O p-orbital to Cr d-orbitals and large relative contribution (83%) of the fast (30 fs) fitting component (κ_1). Cr_3O_6 contains three tri-coordinated Cr atoms and three terminal O atoms. Cr_3O_5 has only two terminal O atoms, resulting in a lower LMCT character. The photoexcited state in Cr_3O_3 has only a 5% LMCT component and its dynamics show a relatively small κ_1 contribution (0.51). The excited states of Cr_3O_3 near 3.1 eV show strong $d \rightarrow p$ and $d \rightarrow s$ excitation on the Cr atoms instead of a strong LMCT character, inconsistent with the moderate κ_1 value (0.56). It is likely that the energies of the LMCT states are overestimated. At a slightly higher absorption energy (calculated at 3.47 eV), there is a 37% LMCT in Cr_3O_4 that agrees with the increased experimental κ_1 value (0.71) and is likely accessed. Cr_3O_5 and Cr_3O_6 both have significant LMCT character of 33 and 46%, respectively, and is reflected in a high proportion of κ_1 (0.70 and 0.83 respectively). Both the LMCT and κ_1 values are slightly larger for Cr_3O_6 than for Cr_3O_5 , in agreement to the described trend.

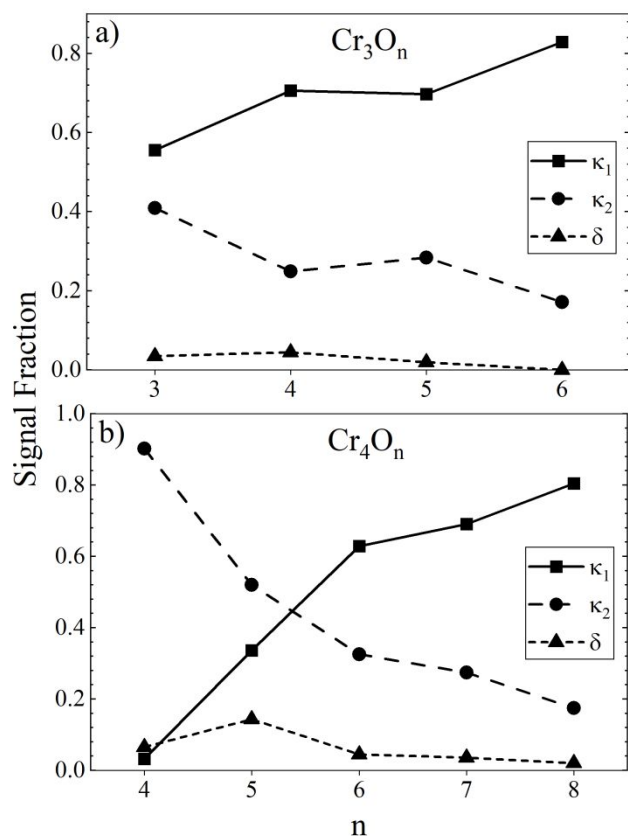


Figure 4: The fractional change in total signal contribution of separate functions for the fast lifetime (κ_1), sub-ps lifetime (κ_2) and the plateau function (δ) for a) Cr_3O_n and b) Cr_4O_n clusters.

Transient signals and structures of Cr_4O_n ($n = 4-8$) clusters are presented in Fig. 5. With four Cr atoms, the lowest energy structures for the clusters transition from a planar configuration associated with the smaller clusters into a compact 3D structure. These clusters also avoid Cr-Cr bonding and do not contain terminal O atoms until Cr_4O_7 , consistent with previous calculations.¹² The lowest energy geometry of neutral Cr_4O_7 and Cr_4O_8 contain one and two terminal O atoms, respectively, resulting in tetracoordinated Cr atoms. This significant change in structural motif is also accompanied by a stark decrease in the relative κ_1 fraction (Fig 4b) obtained for the clusters containing few O atoms ($\text{Cr}_4\text{O}_{4-6}$) compared to the smaller Cr_3O_n clusters. However, the general trend reported in the relative amplitudes of the fitting coefficients for the smaller clusters continues, showing that as the O content increases, the photoexcitation shifts toward increasing LMCT character. The transient signal for Cr_4O_4 is dominated by the τ_2 fitting function ($\kappa_2 = 90\%$). Cr_4O_5 is also dominated by κ_2 (0.52), but also contains a large κ_1 component (0.34). The relative κ_2 contributions decrease almost linearly with O content, while the δ component remains relatively negligible. Cr_4O_7 and Cr_4O_8 have a larger relative κ_2 and δ contribution that is consistent with the smaller clusters.

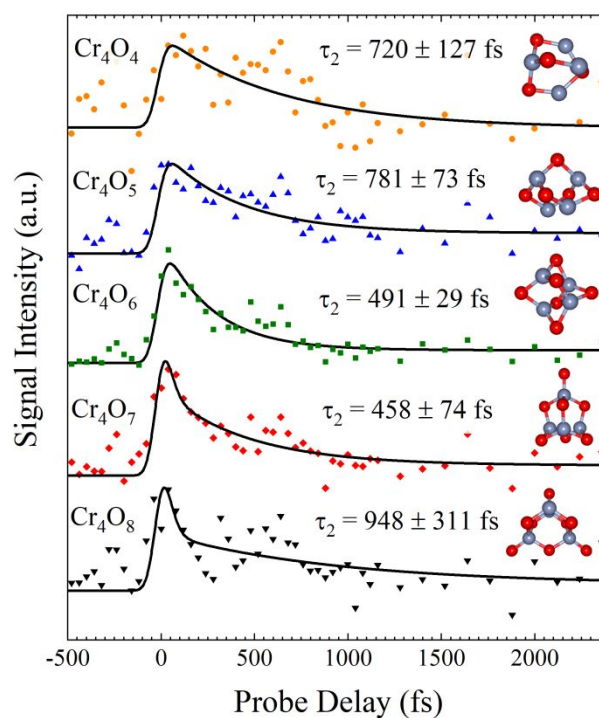


Figure 5: Transient signal of neutral Cr_4O_n ($n = 4-8$) following pump-probe ionization, with stable geometries and lifetimes above each signal.

Although the oxidation state in Cr_2O_n clusters changes by integer values with sequential addition of each O atom, the change in oxidation state of each Cr with each O in larger clusters is smaller (non-integer values). This experiment confirms that the trend reported in Cr_2O_n clusters³⁸ extends into larger sizes, despite the LMCT component of the excited state transition for the Cr_4O_n series is not as pronounced as it is for the smaller clusters. This suggests that photoexcitation for larger clusters may be more of a d-d transition, and therefore not exhibit as strong of an e-e scattering mechanism. Therefore, the extremely fast e-e scattering relaxation phenomenon may be most pronounced in planar structures.

3.3 Size Effects on Excited State Lifetimes

Following vertical photoexcitation, the clusters undergo adiabatic relaxation, where additional degrees of vibrational freedom may improve the larger cluster's propensity to return to the ground state as vibrationally hot species. Only the smallest clusters of CrO_n and Cr_2O_n contain a significant population attributed to a long-lived excited state, while the larger sized clusters (Cr_3O_n and Cr_4O_n) do not and likely dissipate the electronic energy into additional degrees of vibrational motion. The relative δ values decrease with increased size, showing that long-lived excited states are increasingly accessed in smaller clusters.

The sub-ps excited state lifetimes (τ_2) recorded for all neutral clusters are compared in Fig. 6. The CrO_n clusters slightly decrease with oxidation from 395 ± 38 fs for Cr to 333 ± 52 fs for CrO_2 , suggesting that the presence of O atoms enables a faster relaxation. Like the CrO_n cluster series, the sub-ps excited state lifetimes of the Cr_3O_n ($n = 3-6$) clusters slightly decrease in

lifetime with additional O atoms, changing from 770 ± 95 fs for Cr_3O_3 and gradually reducing to 530 ± 94 fs for Cr_3O_6 . Unlike the clusters that contain an odd number of Cr atoms, the transient dynamics for Cr_2O_n and Cr_4O_n clusters do not show an obvious trend in their sub-ps lifetimes and highlights that sub-nm scale materials represent the size regime of non-scalable properties. In each cluster series, the $\text{Cr}_n\text{O}_{2n-3}$ clusters exhibit longer lifetimes. As the clusters gain O atoms, the sub-ps lifetimes decrease until reaching $(\text{CrO}_2)_n$ stoichiometry which contains conflicting results. Although CrO_2 and Cr_3O_6 contain the shortest lifetimes within their respective cluster series, Cr_2O_4 and Cr_2O_8 display long lifetimes and therefore break the trend. It should be noted that the small ion signal recorded for Cr_4O_8 produces a large error bar, but consistently exhibits the longest lifetime measured (948 ± 311 fs).

The sub-ps lifetimes measured for the $(\text{CrO}_2)_n$ stoichiometries increase with size, beginning with a lifetime of 333 ± 26 fs for CrO_2 and reaching a lifetime of 948 ± 311 fs for Cr_4O_8 . This cluster series displays efficient relaxation on (10s of fs) timescales and exhibits a negligible δ contribution (Table 1). Our calculations show the lowest energy structures for each of the $(\text{CrO}_2)_n$ clusters possess terminally bound O atoms with double bonds. The presence of terminal O atoms seems particularly important for the excited state transient dynamics to display a prominent κ_1 contribution, and raises the possibility that the rapid relaxation is related to internal conversion, which is known to be facilitated by the vibronic motions of terminal O atoms.^{40,55} Vibrationally mediated internal conversion and e-e relaxation are a challenge to disentangle because the addition of terminal O atoms increases the cluster's vibrational degrees of freedom, but also increase the ligand character of the occupied electron orbitals involved in photoexcitation. With increasing oxidation, the accessible occupied orbitals shift onto O atoms, while the unoccupied orbitals remain on the Cr atoms, enabling a higher LMCT character. If vibrational motion of the terminal Cr=O bonds is driving the fast relaxation, then a sharp contrast in behavior is expected with the onset of terminal Cr=O bonds, which does not align with the experimental data. The Cr_3O_n series varies between containing zero and three terminal O atoms, and yet the κ_1 contribution remains large. Similarly, the $\text{Cr}_4\text{O}_6 - \text{Cr}_4\text{O}_8$ clusters contain similar κ_1 values but transitions between containing zero and two terminal O atoms. A significant change in relaxation mechanism is not observed with the number of terminal O atoms, but instead a gradual change in the values of the κ_1 contribution closely aligns with the LMCT character as represented in Table 1. Therefore, the κ_1 magnitude is related to the electronic character, and not the geometric structure and number of O atoms. The terminal O atoms facilitate e-e relaxation by increasing the LMCT character of the accessible electronic excitation, but do not inherently drive relaxation through internal conversion directly.

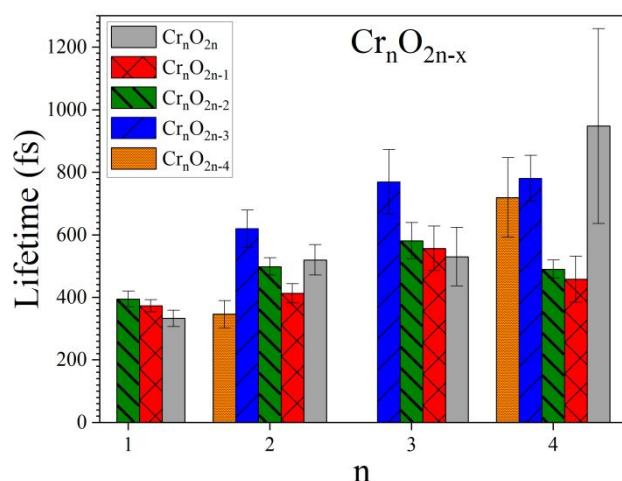


Figure 6: Sub-ps lifetimes (τ_2) for all neutral $\text{Cr}_n\text{O}_{2n-x}$ clusters ($n = 1-4$), with the Cr_nO_{2n} (solid gray), $\text{Cr}_n\text{O}_{2n-1}$ (red cross), $\text{Cr}_n\text{O}_{2n-2}$ (green back slash), $\text{Cr}_n\text{O}_{2n-3}$ (blue forward slash), and $\text{Cr}_n\text{O}_{2n-4}$ (orange dotted) series shown.

These results show that the metallic behavior of the excited states of sub-nanometer chromium oxide clusters increases nearly linearly with oxidation. This tunable behavior is not just a rare case of the Cr_2O_n clusters but is revealed to be a general trend that extends to larger, more complex clusters and will likely continue into even larger clusters. These properties can be employed to design new chromium oxide materials that capitalize on the tailored excited state dynamics through selected O content. Most importantly, these results suggest that O deficiencies will cause large changes in chromium oxide material's ultrafast response and properties.

4. Conclusion

Neutral sub-nm chromium oxide clusters were produced in the gas-phase and their low-lying excited state transient dynamics were measured using a 3.1 eV pump photon and strong-field ionization. The transient dynamics show trends related to size, oxidation, and relate strongly to the percent LMCT character. DFT calculations were used to relate the changes in the transient dynamics to the nature of the photoexcitation. Specifically, TD-DFT calculations reveal that the systematic oxidation of chromium oxide clusters results in a near linear shift in LMCT character (O-2p to Cr-3d) matching the increase in κ_1 for each cluster series. The increase in the contribution of the 10s of fs relaxation mechanism (metallic behavior) for chromium oxide clusters with oxidation is counterintuitive and is explained as approaching the half-metal stoichiometry and behavior of bulk CrO_2 . Smaller clusters with less O character have a greater propensity to possess long-lived excited states. The change in the fitting function contributions reveal that LMCT excitations relax on a nearly instantaneous timescale and d-d excitations relax on a slower sub-ps timescale. The information provided here will assist in understanding electronic transition effects on excited state lifetimes in chromium oxides as they grow, inevitably leading to chromium materials of increased reactivity. Therefore, the half-

metal behavior is shown at the molecular level and suggests that the wide variety of cluster geometries and structures will enable new molecular scale spintronic materials to be developed.

Author Contributions

SGS and JMG designed the experiments. JMG performed the ultrafast pump-probe spectroscopy, SGS performed the theoretical calculations, and SGS and JMG wrote the manuscript together.

Conflicts of interest

There are no conflicts to declare

Acknowledgements

We gratefully acknowledge support from ASU Lightworks. J.G also acknowledges support from Western Alliance to Expand Student Opportunities (WAESO) Louis Stokes Alliance for Minority Participation (LSAMP) Bridge to Doctorate (BD) National Science Foundation (NSF) Grant No. HRD-1702083.

References

- 1 L. A. Büldt and O. S. Wenger, Chromium complexes for luminescence, solar cells, photoredox catalysis, upconversion, and phototriggered NO release, *Chem. Sci.*, 2017, **8**, 7359–7367.
- 2 J. B. Griffin and P. B. Armentrout, Guided ion beam studies of the reactions of Cr_n^+ ($n=1-18$) with CO_2 : Chromium cluster oxide bond energies, *J. Chem. Phys.*, 1998, **108**, 8075–8083.
- 3 I. Rivalta, N. Russo and E. Sicilia, Methane activation by chromium oxide cations in the gas phase: A theoretical study, *J. Comput. Chem.*, 2006, **27**, 174–187.
- 4 E. V. Shah and D. R. Roy, Magnetic switching in Cr_x ($x = 2-8$) and its oxide cluster series, *J. Magn. Magn. Mater.*, 2018, **451**, 32–37.
- 5 G. M. Müller, J. Walowski, M. Djordjevic, G. X. Miao, A. Gupta, A. V Ramos, K. Gehrke, V. Moshnyaga, K. Samwer, J. Schmalhorst, A. Thomas, A. Hütten, G. Reiss, J. S. Moodera and M. Münzenberg, Spin polarization in half-metals probed by femtosecond spin excitation, *Nat. Mater.*, 2009, **8**, 56–61.
- 6 K. H. Heffernan, S. Yu, S. Deckoff-Jones, X. Zhang, A. Gupta and D. Talbayev, Role of spin fluctuations in the conductivity of CrO_2 , *Phys. Rev. B*, 2016, **93**, 165143.
- 7 I. V Solov'yev, I. V Kashin and V. V Mazurenko, Mechanisms and origins of half-metallic ferromagnetism in CrO_2 , *Phys. Rev. B - Condens. Matter Mater. Phys.*, 2015, **92**, 144407.
- 8 D. E. Bergeron, A. W. Castleman, N. O. Jones and S. N. Khanna, Stable Cluster Motifs for Nanoscale Chromium Oxide Materials, *Nano Lett.*, 2004, **4**, 261–265.
- 9 T. Satoh, B. B. Van Aken, N. P. Duong, T. Lottermoser and M. Fiebig, Ultrafast spin and lattice dynamics in antiferromagnetic Cr_2O_3 , *Phys. Rev. B - Condens. Matter Mater. Phys.*, 2007, **75**, 1–6.
- 10 M. Fiebig, N. P. Duong, T. Satoh, B. B. Van Aken, K. Miyano, Y. Tomioka and Y. Tokura, Ultrafast magnetization dynamics of antiferromagnetic compounds, *J. Phys. D: Appl. Phys.*, 2008, **41**, 164005.
- 11 F. Guo, N. Zhang, W. Jin and J. Chang, Model of ultrafast demagnetization driven by spin-orbit coupling in a photoexcited antiferromagnetic insulator Cr_2O_3 , *J. Chem. Phys.*, 2017, **146**, 244502.
- 12 L. N. Pham, P. Claes, P. Lievens, L. Jiang, T. Wende, K. R. Asmis, M. T. Nguyen and E. Janssens, Geometric Structures and Magnetic Interactions in Small Chromium Oxide Clusters, *J. Phys. Chem. C*, 2018, **122**, 27640–27647.
- 13 C. W. Bauschlicher, C. J. Nelin and P. S. Bagus, Transition metal oxides: CrO, MoO, NiO, PdO, AgO, *J. Chem. Phys.*, 1984, **82**, 3265–3276.
- 14 G. A. Cooper, A. S. Gentleman, A. Iskra and S. R. Mackenzie, Photofragmentation dynamics and dissociation energies of MoO and CrO, *J. Chem. Phys.*, 2017, **147**, 13921.
- 15 J. J. Sorensen, E. Tieu, A. Sevy, D. M. Merriles, C. Nielson, J. C. Ewigeleben and M. D. Morse, Bond dissociation energies of transition metal oxides: CrO, MoO, RuO, and RhO, *J. Chem. Phys.*, 2020, **153**, 74303.
- 16 T. C. Devore and J. L. Gole, Formation of the low-lying electronic states of CrO in highly exothermic reactive oxidation. Assessment of new states and partial resolution of previous observations, *Chem. Phys.*, 1989, **133**, 95–102.
- 17 A. S.-C. Cheung, W. Zyrnicki and A. J. Merer, Fourier transform spectroscopy of CrO: Rotational analysis of the $A^5\Sigma-X^5\Pi$ (0,0) band near 8000 cm^{-1} , *J. Mol. Spectrosc.*, 1984, **104**, 315–336.
- 18 G. V. Chertihin, W. D. Bare and L. Andrews, Reactions of laser-ablated chromium atoms with dioxygen. Infrared spectra of CrO, OCrO, CrOO, CrO_3 , $\text{Cr}(\text{OO})_2$, Cr_2O_2 , Cr_2O_3 and Cr_2O_4 in solid argon, *J. Chem. Phys.*, 1998, **107**, 2798.
- 19 P. G. Wenthold, R. F. Gunion and W. C. Lineberger, Ultraviolet negative-ion photoelectron spectroscopy of the chromium oxide negative ion, *Chem. Phys. Lett.*, 1996, **258**, 101–106.
- 20 P. G. Wenthold, K.-L. Jonas and W. C. Lineberger, Ultraviolet photoelectron spectroscopy of the chromium dioxide negative ion, *J. Chem. Phys.*, 1997, **106**, 9961–9962.
- 21 P. F. Souter and L. Andrews, A Spectroscopic and Theoretical Study of the Reactions of Group 6 Metal Atoms with Carbon Dioxide, *J. Am. Chem. Soc.*, 1997, **119**, 7350–7360.
- 22 M. Zhou and L. Andrews, Infrared spectra and density functional calculations of the CrO_2^- , MoO_2^- , and WO_2^- molecular anions in solid neon, *J. Chem. Phys.*, 1999, **111**, 4230–4238.
- 23 G. L. Gutsev, P. Jena, H. J. Zhai and L. S. Wang, Electronic structure of chromium oxides, CrO_n^- and CrO_n ($n=1-5$) from photoelectron spectroscopy and density functional theory calculations, *J. Chem. Phys.*, 2001, **115**, 7935–7944.
- 24 F. Grein, DFT and MRCI studies on ground and excited states of CrO_2 , *Chem. Phys.*, 2008, **343**, 231–240.

- 25 K. Tono, A. Terasaki, T. Ohta and T. Kondow, Chemically induced ferromagnetic spin coupling: Electronic and geometric structures of chromium-oxide cluster anions, Cr_2O_n^- ($n=1-3$), studied by photoelectron spectroscopy, *J. Chem. Phys.*, 2003, **119**, 11221–11227.
- 26 B. Reddy, S. Khanna and C. Ashman, Oscillatory magnetic coupling in Cr_2O_n ($n=1-6$) clusters, *Phys. Rev. B - Condens. Matter Mater. Phys.*, 2000, **61**, 5797–5801.
- 27 G. L. Gutsev, K. V. Bozhenko, L. G. Gutsev, A. N. Utenyshev and S. M. Aldoshin, Transitions from stable to metastable states in the Cr_2O_n and Cr_2O_n^- series, $n = 1-14$, *J. Phys. Chem. A*, 2017, **121**, 845–854.
- 28 H. J. Zhai and L. S. Wang, Probing the electronic properties of dichromium oxide clusters Cr_2O_n^- ($n=1-7$) using photoelectron spectroscopy, *J. Chem. Phys.*, 2006, **125**, 164315.
- 29 K. Tono, A. Terasaki, T. Ohta and T. Kondow, Chemical Control of Magnetism: Oxidation-Induced Ferromagnetic Spin Coupling in the Chromium Dimer Evidenced by Photoelectron Spectroscopy, *Phys. Rev. Lett.*, 2003, **90**, 133402.
- 30 Q. Q. Zhang, Y. Zhao, Y. Gong and M. Zhou, Matrix isolation infrared spectroscopic and theoretical study of dinuclear chromium oxide clusters: Cr_2O_n ($n = 2, 4, 6$) in solid argon, *J. Phys. Chem. A*, 2007, **111**, 9775–9780.
- 31 V. E. Bondybey and J. H. English, Electronic structure and vibrational frequency of Cr_2 , *Chem. Phys. Lett.*, 1983, **94**, 443–447.
- 32 S. Veliah, K. H. Xiang, R. Pandey, J. M. Recio and J. M. Newsam, Density functional study of chromium oxide clusters: Structures, bonding, vibrations, and stability, *J. Phys. Chem. B*, 1998, **102**, 1126–1135.
- 33 H. J. Zhai, S. Li, D. A. Dixon and L. S. Wang, Probing the electronic and structural properties of chromium oxide clusters (CrO_3) $_n^-$ and (CrO_3) $_n$ ($n = 1-5$): Photoelectron spectroscopy and density functional calculations, *J. Am. Chem. Soc.*, 2008, **130**, 5167–5177.
- 34 T. Morisato, N. O. Jones, S. N. Khanna and Y. Kawazoe, in *Computational Materials Science*, 2006, vol. 35, pp. 366–370.
- 35 K. S. Molek, Z. D. Reed, A. M. Ricks and M. A. Duncan, Photodissociation of chromium oxide cluster cations, *J. Phys. Chem. A*, 2007, **111**, 8080–9.
- 36 I. Kumari, S. Gupta and N. Goel, A DFT based investigation of NO oxidation by $(\text{CrO}_3)_3$ cluster, *Comput. Theor. Chem.*, 2016, **1091**, 107–114.
- 37 R. Moriyama, R. Sato, M. Nakano, K. Ohshimo and F. Misaizu, Geometrical Structures of Gas Phase Chromium Oxide Cluster Anions Studied by Ion Mobility Mass Spectrometry, *J. Phys. Chem. A*, 2017, **121**, 5605–5613.
- 38 J. M. Garcia and S. G. Sayres, Increased Excited State Metallicity in Neutral Cr_2O_n Clusters ($n < 5$) upon Sequential Oxidation, *J. Am. Chem. Soc.*, 2021, **143**, 15572–15575.
- 39 W. C. Wiley and I. H. McLaren, Time-of-Flight Mass Spectrometer with Improved Resolution, *Rev. Sci. Instrum.*, 1955, **26**, 1150–1157.
- 40 J. M. Garcia, L. F. Heald, R. E. Shaffer and S. G. Sayres, Oscillation in Excited State Lifetimes with Size of Subnanometer Neutral $(\text{TiO}_2)_n$ Clusters Observed with Ultrafast Pump–Probe Spectroscopy, *J. Phys. Chem. Lett.*, 2021, **12**, 4098–4103.
- 41 J. M. Garcia, R. E. Shaffer and S. G. Sayres, Ultrafast pump-probe spectroscopy of neutral Fe_nO_m clusters ($n, m < 16$), *Phys. Chem. Chem. Phys.*, 2020, **22**, 24624–24632.
- 42 T. E. Dermota, D. P. Hydutsky, N. J. Bianco and A. W. Castleman Jr., Photoinduced ion-pair formation in the $(\text{HI})_m(\text{H}_2\text{O})_n$ cluster system, *J. Chem. Phys.*, 2005, **123**, 214308.
- 43 M. J. Frisch, G. W. Trucks, H. B. Schlegel, G. E. Scuseria, M. A. Robb, J. R. Cheeseman, G. Scalmani, V. Barone, B. Mennucci, G. A. Petersson, H. Nakatsuji, M. Caricato, X. Li, H. P. Hratchian, A. F. Izmaylov, J. Bloino, G. Zheng, J. L. Sonnenberg, M. Hada, M. Ehara, K. Toyota, R. Fukuda, J. Hasegawa, M. Ishida, T. Nakajima, Y. Honda, O. Kitao, H. Nakai, T. Vreven, J. A. Montgomery Jr., J. E. Peralta, F. Ogliaro, M. Bearpark, J. J. Heyd, E. Brothers, K. N. Kudin, V. N. Staroverov, R. Kobayashi, J. Normand, K. Raghavachari, A. Rendell, J. C. Burant, S. S. Iyengar, J. Tomasi, M. Cossi, N. Rega, J. M. Millam, M. Klene, J. E. Knox, J. B. Cross, V. Bakken, C. Adamo, J. Jaramillo, R. Gomperts, R. E. Stratmann, O. Yazyev, A. J. Austin, R. Cammi, C. Pomelli, J. W. Ochterski, R. L. Martin, K. Morokuma, V. G. Zakrzewski, G. A. Voth, P. Salvador, J. J. Dannenberg, S. Dapprich, A. D. Daniels, O. Farkas, J. B. Foresman, J. V. Ortiz, J. Cioslowski and D. J. Fox, Gaussian Inc. Wallingford CT, 2016.
- 44 J. P. Perdew and Y. Wang, Accurate and simple analytic representation of the electron-gas correlation energy, *Phys. Rev. B*, 1992, **45**, 13244–13249.
- 45 M. J. G. Peach, P. Benfield, T. Helgaker and D. J. Tozer, Excitation energies in density functional theory: An evaluation and a diagnostic test, *J. Chem. Phys.*, 2008, **128**, 044118.
- 46 T. Yanai, D. P. Tew and N. C. Handy, A new hybrid exchange-correlation functional using the Coulomb-attenuating method (CAM-B3LYP), *Chem. Phys. Lett.*, 2004, **393**, 51–57.
- 47 E. Berardo, H. S. Hu, H. J. J. Van Dam, S. A. Shevlin, S. M. Woodley, K. Kowalski and M. A. Zwijnenburg, Describing excited state relaxation and localization in TiO_2 nanoparticles using TD-DFT, *J. Chem. Theory Comput.*, 2014, **10**, 5538–5548.
- 48 E. Berardo, H. S. Hu, S. A. Shevlin, S. M. Woodley, K. Kowalski and M. A. Zwijnenburg, Modeling excited states in TiO_2 nanoparticles: On the accuracy of a TD-DFT based description, *J. Chem. Theory Comput.*, 2014, **10**, 1189–1199.
- 49 F. Rabilloud, UV-visible absorption spectra of metallic clusters from TDDFT calculations, *Eur. Phys. J. D*, 2013, **67**, 1–5.
- 50 F. Aubriet and J. F. Muller, About the Atypical behavior of CrO_3 , MoO_3 , and WO_3 during their UV laser ablation/ionization, *J. Phys. Chem. A*, 2002, **106**, 6053–6059.

- 51 N. Pontius, P. S. Bechthold, M. Neeb and W. Eberhardt, Time-resolved photoelectron spectra of optically excited states in Pd₃⁻, *J. Electron Spectros. Relat. Phenomena*, 2001, **114–116**, 163–167.
- 52 N. Pontius, G. Lüttgens, P. S. Bechthold, M. Neeb and W. Eberhardt, Size-dependent hot-electron dynamics in small Pd_n⁻ clusters, *J. Chem. Phys.*, 2001, **115**, 10479–10483.
- 53 N. Pontius, P. S. Bechthold, M. Neeb and W. Eberhardt, Ultrafast Hot-Electron Dynamics Observed in Pt₃⁻ Using Time-Resolved Photoelectron Spectroscopy, *Phys. Rev. Lett.*, 2000, **84**, 1132–1135.
- 54 J. Heinzlmann, A. Koop, S. Proch, G. F. Ganteför, R. Łazarski and M. Sierka, Cage-Like nanoclusters of ZnO probed by time-resolved photoelectron spectroscopy and theory, *J. Phys. Chem. Lett.*, 2014, **5**, 2642–2648.
- 55 W. T. Peng, B. S. Fales, Y. Shu and B. G. Levine, Dynamics of recombination: Via conical intersection in a semiconductor nanocrystal, *Chem. Sci.*, 2018, **9**, 681–687.